CHAPTER 216

VERTICAL STRUCTURE OF THE NEARSHORE CURRENT AT DELILAH: MEASURED AND MODELED

Jane McKee Smith[1], Ib A. Svendsen[2], and Uday Putrevu[3]

ABSTRACT: Comprehensive field measurements were made of the vertical current structure on a barred beach profile at the DELILAH project during October of 1990. The current was measured with five electromagnetic current meters mounted on a mobile sled which was stationed at three to eight cross-shore positions. The incident directional wave spectra, bathymetry, tide, wind, and cross-shore wave transformation were also measured. A numerical model was developed to calculate the random wave transformation based on the model of Dally, Dean, and Dalrymple (1985) (Larson and Kraus 1991) and the local vertical current structure (Putrevu and Svendsen 1991). The model predicted the shape of the current profiles well with a root-mean-square error in velocity of 5.9 cm/sec. The model tended to underpredict the velocity over the bar crest.

INTRODUCTION

Predicting the vertical structure of the cross-shore current is a critical step to advancing the modeling of beach evolution, especially the response of the beach profile to storms, the post-storm profile recovery, and the development and movement of bars. The cross-shore currents have also been shown to be important in describing the mixing for longshore currents (Putrevu and Svendsen 1992, Svendsen and Putrevu 1992b). The lack of high-quality field measurements of the vertical current structure has been a hinderance to the development and validation of cross-shore current models.

In October of 1990, a comprehensive field experiment was performed at the U.S. Army Engineer Waterways Experiment Station, Coastal Engineering Research Center

[1]Res. Hyd. Engr., US Army Engr. Waterways Exp. Sta., Coast. Engrg. Res. Center, 3909 Halls Ferry Rd., Vicksburg, MS 39180-6199, USA.
[2]Prof., Dept. of Civil Engrg., Univ. of Delaware, Newark, DE 19716, USA.
[3]Res. Assoc., Dept. of Civil Engrg., Univ. of Delaware, Newark, DE 19716, USA.

(CERC), Field Research Facility (FRF) in Duck, NC, to measure the wind- and wave-forced three-dimensional nearshore hydrodynamics. The DELILAH (Duck Experiment on Low-frequency and Incident-band Longshore and Across-shore Hydrodynamics) experiment was a cooperative project involving researchers from CERC, Naval Postgraduate School, Naval Research Lab, Oregon State University, Quest Integrated, Inc., Scripps Institution of Oceanography, University of California at Santa Cruz, and Washington State University.

The hydrodynamic data collected at DELILAH were used to refine and verify a numerical model developed to calculate the vertical variation of the cross-shore current. The purpose of this paper is to describe the DELILAH field measurements and to describe the application of these data to evaluate the numerical model.

DELILAH FIELD PROJECT

The core of the DELILAH field project was a fixed array of 19 electromagnetic current meters deployed in one cross-shore array and two longshore arrays to the north of the FRF pier. The cross-shore array consisted of nine sensor positions, extending from the shoreline to 350 m offshore (4-m depth). A pressure gage was deployed along with a current meter at each position in the cross-shore array. The longshore arrays were positioned approximately on the bar crest and in the trough of the beach profile. The longshore arrays were approximately 200 m long.

The bathymetry adjacent to the current meter arrays (340 m by 600 m area) was surveyed daily during the experiment. Accurate surveying was accomplished with a special self-contained vehicle, the CRAB (Coastal Research Amphibious Buggy), that drove along survey transects (Birkemeier and Mason 1984). The position and elevation of the CRAB was determined with a Geodimeter auto-tracking electronic total station. Fig. 1 shows an example of the bathymetry surveyed on 19 October 1990. The bathymetry was generally homogeneous in the longshore direction during the cross-shore current measurements, with a linear bar approximately 100 m offshore. Offshore directional wave spectra were measured with an array of sixteen pressure gages at the 8-m depth contour. Spectra were measured every 3 hours during the experiment and provide offshore boundary conditions for wave forcing of the current model. Fig. 2 shows the two-dimensional spectrum measured on 19 October 1990 at 1300. In Fig. 2, the x-axis is the frequency, f, the y-axis is the wave direction (measured counter-clockwise from shore normal), θ, and the z-axis is the energy density, S. Over-water winds and tidal elevation were measured at the FRF pier.

CROSS-SHORE CURRENT MEASUREMENTS

The vertical structure of the current was measured with a vertical array of five electromagnetic current meters mounted on a mobile sled. The meters were mounted at elevations 0.35 m, 0.6 m, 1.0 m, 1.35 m, and 1.75 m above the bed on a vertically sloping beam. The beam was parallel to the shoreline, so the meters were aligned in the cross-shore. The meters were spread over a longshore distance of approximately 3.5 m. The sled was always deployed so that the lower end of the beam was in the updrift direction of the longshore current to reduce interference of the flow. A common timing pulse was used for all the current meters to reduce interference between instruments for this close proximity deployment. The meters measured the longshore and cross-shore components of the
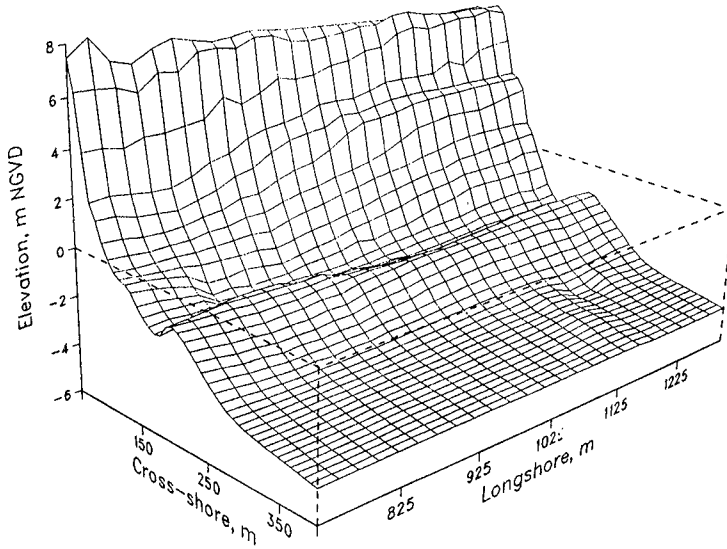
Figure 1. Bathymetry for 19 October 1990.
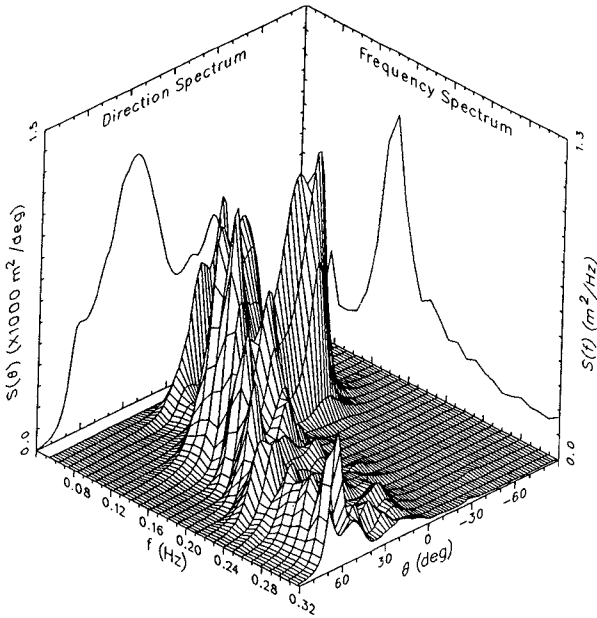
Figure 2. Two-dimensional spectrum for 19 October 1990.

current. The sled was also instrumented with a pressure gage, a resistance wave staff, and an anemometer.

During the experiment, the sled was towed offshore of the breaker zone by the CRAB to a depth of approximately 3 m. The sled was then pulled back to shore with a fork lift in steps of 20 m. At each sled position, data were collected for 34 minutes. The collection period of 34 minutes was selected to balance the competing needs for long time series for stable statistics and short total time for the sled deployment to ensure stationarity of the incident waves. All current data presented are 34 minute averages. The data were telemetered to shore for real-time data quality checking. Three to eight cross-shore positions were occupied during each of eight deployments. The position and orientation of the sled were recorded using an electronic total station which sighted two prisms located on the sled mast.

The sled was deployed near the cross-shore array of current meters and pressure gages. The fixed array gages provided background data on the horizontal structure of the hydrodynamics and on the stationarity of the waves and currents. Fig. 3 shows an example of the vertical structure of the cross-shore current measured during DELILAH. The vectors in Fig. 3 represent cross-shore current magnitude and direction measured at six sled positions on 19 October 1990. The solid lines in Fig. 3 represent the survey datum and bottom profile (d). Sled measurements were made during the final six days of the DELILAH experiment. Incident waves during these days provided a variety of conditions with wave heights of 0.5 to 1.5 m, peak spectral periods of 5 to 15 sec, wind speeds of 5 to 15 m/sec, and wave directions both north and south of shorenormal. The maximum time-averaged current velocities exceeded 0.5 m/sec during measurements with the sled.
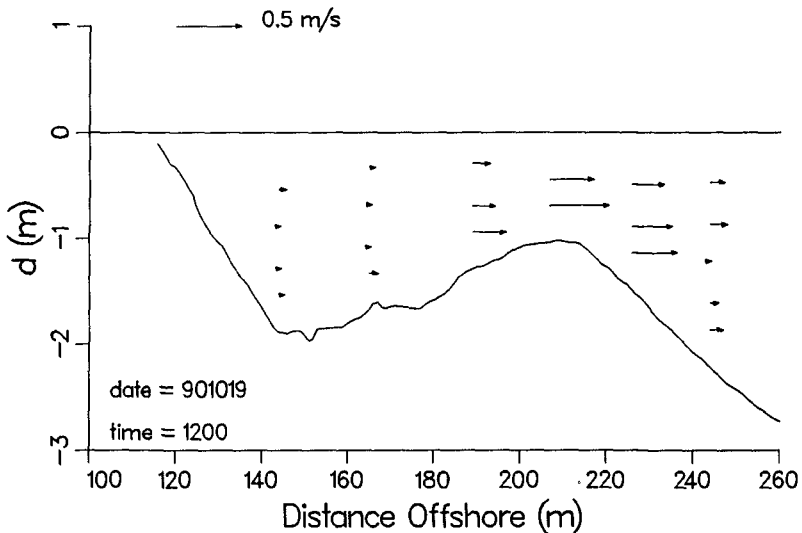
Figure 3. Cross-shore current velocities measured during DELILAH (19 Oct 1990).

NUMERICAL MODEL

The numerical model consists of two parts, a random wave transformation model and a model of the cross-shore flow. The wave transformation model provides the cross-shore gradient in wave height and the cross-shore variation in the mean water level which are the driving forces of the cross-shore flow. The models assume longshore homogeneity, linear wave theory, and steady-state wave forcing. Wave-current and wave-wave interactions and long wave generation are neglected.

Wave Transformation

The random wave transformation model is based on the decay and reformation model of Dally, Dean, and Dalrymple (1985) as applied to random waves by Larson and Kraus (1991). The Dally, Dean, and Dalrymple model has been shown to be less accurate than other models for predicting wave setup (Svendsen and Putrevu 1992a), the main driving force for the undertow, but it was chosen because it includes a mechanism for breaking waves to reform in the trough shoreward of the longshore bar. The input wave parameters are the root-mean-square wave height (H_{rms}), peak wave period, and peak wave direction measured at the linear array in a depth of 8 m. One hundred wave heights were randomly chosen from a Rayleigh distribution specified by H_{rms}. Each of the one hundred wave heights was transformed across the beach profile, assuming the same period and incident direction for each wave, according to

$$\frac{d(F\cos\theta)}{dx} = \frac{\kappa}{d}(F - F_s) \tag{1}$$

where

F = $0.125\,\rho g H^2 C_g$, energy flux
ρ = water density
g = gravitational acceleration
H = individual wave height
C_g = group velocity
θ = wave direction, relative to shore normal
x = cross-shore coordinate, positive seaward
d = total water depth (still-water plus setup)
F_s = stable energy flux associated with the stable wave height, H_s
H_s = Γd, with $\Gamma = 0.4$ (Dally, Dean, and Dalrymple 1985)

The parameter κ is zero seaward of wave breaking, with breaking specified by a height to depth ratio less than 0.78. At incipient wave breaking, κ is set to 0.15. Wave breaking ceases when the broken height is less than H_s, and κ is reset to zero. The wave directions are determined by Snell's law. The wave parameters were calculated at a 1-m cross-shore spaced grid using an explicit finite difference solution. The H_{rms} was calculated at each grid point from the 100 individual wave heights.

The wave setup, $\overline{\eta}$, is calculated from the time- and depth-averaged cross-shore momentum equation

$$\rho g (h + \overline{\eta}) \frac{d\overline{\eta}}{dx} = -\frac{dS_{xx}}{dx} - \rho_a C_w W W_x \qquad (2)$$

where

h = still-water depth (including the tide)
ρ_a = air density
C_w = wind drag coefficient
W = wind speed
W_x = cross-shore component of the wind velocity
S_{xx} = cross-shore component of radiation stress

The two driving forces of the setup are the gradient in radiation stress and the cross-shore wind stress. The radiation stress is calculated using linear wave theory (Longuet-Higgins and Stewart 1964) based on H_{rms}. Considering the simplifying assumptions used to represent the random wave field, a more sophisticated evaluation of the radiation stress (Svendsen and Putrevu 1992a) is not justified. The wind drag coefficient given by the WAMDI Group (1988) is adopted in the model (C_w = .0012875 for W < 7.5 m/sec; C_w = 0.0008 + 0.000065 W for W > 7.5 m/sec). The bed shear stress is known to be small and is neglected in Eq. 2. One iteration was required between the calculation of the wave height transformation and the wave setup.

The Cross-shore Current

The vertical variation of the current is modeled with a three-layer approach (Hansen and Svendsen 1984; Stive and de Vriend 1987; Svendsen and Hansen 1988). The velocity distribution in the central layer is calculated as a local solution of the depth-dependent, cross-shore momentum equation with the surface and lower layers contributing boundary conditions. The central layer extends from the bottom boundary layer to the trough level. The lower layer, the bottom boundary layer, relates the near bottom current velocity to the mean bottom stress (Svendsen and Putrevu 1990). The upper layer contributes the mass flux which is balanced by the undertow in the central layer. In the present application, it is assumed that no net cross-shore flow exists, i.e., the mass flux above the trough balances the undertow. Forcing for the vertical variation includes gradients in radiation stress, mean current, and setup. The horizontal gradient terms in the model are calculated from the depth-integrated, one-dimensional model described above.

The vertical current structure is calculated from a double integration of the depth-dependent, cross-shore momentum equation (Putrevu and Svendsen 1991)

$$U(\zeta) = U_b + \alpha \frac{\zeta^2}{2 \nu_{tz}} + \frac{\tau_{bx} \zeta}{\rho \nu_{tz}} \qquad (3)$$

where

ζ = vertical coordinate, measured positive from the bottom
U = cross-shore velocity at elevation ζ

τ_{bx} = bottom stress (Eq. 4)
U_b = bottom velocity (Eq. 5)
α = driving force for the undertow (Eq. 6)
ν_{tz} = eddy viscosity (Eq. 8)

In deriving Eq. 3 both α and ν_{tz} have been assumed constant over depth. The bottom boundary condition includes the bottom stress

$$\tau_{bx} = \rho \frac{2}{\pi} f_w u_0 U_b \qquad (4)$$

where

f_w = bottom friction factor
u_0 = wave orbital velocity at the bottom

and the bottom velocity. The bottom velocity is determined from the depth integration of Eq. 3 with Eq. 4 substituted for the bottom stress

$$U_b = \frac{\overline{U} - \dfrac{\alpha d_t^2}{6\nu_{tz}}}{1 + \dfrac{f_w d_t u_0}{2\pi \nu_{tz}}} \qquad (5)$$

where

d_t = depth to trough level
$\overline{U}$ = mean undertow velocity (Eq. 7)

The driving force in Eqs. 3 and 5 is given by

$$\alpha = g \frac{d\overline{\eta}}{dx} + \overline{U} \frac{d\overline{U}}{dx} + u_w \frac{du_w}{dx} + \frac{\rho_a}{\rho} \frac{C_w W W_x}{d_t} \qquad (6)$$

where u_w is the depth-averaged wave velocity and ρ_a is the density of air. The boundary condition from the upper layer is the mass transport above the trough elevation, which balances the undertow. The mass transport is proportional to CH^2/d, where C is the wave celerity, and the constant of proportionality was found to be approximately -0.3 based on the undertow measurements. The mean undertow in Eq. 5 is given by

$$\overline{U} = \frac{0.3\sqrt{g(h+\overline{\eta})}\, H^2 \cos\theta}{(h+\overline{\eta})^2} \qquad (7)$$

In the numerical computations we have used the same eddy viscosity at all depths, given by

$$v_{tz} = 0.05 \sim 0.01 \sqrt{g(h + \overline{\eta})_b} (h + \overline{\eta})_b \qquad (8)$$

where the subscript b indicates incipient breaking conditions. In laboratory experiments on a plane beach, v_{tz} has been found to vary as $h\sqrt{gh}$. The simplification of constant v_{tz} is chosen because the depth over the region of the DELILAH measurements varies only between 1.2 and 2.2 m, and little information is available about the variation of v_{tz} under field conditions.

MODEL RESULTS

The model was applied to the 8 cases of DELILAH sled data. The results from 3 cases are shown in Figs. 4 through 9. These cases were selected because they cover a variety of conditions with the largest number of sled positions. These cases are typical of the conditions and measurements during the final week of DELILAH. Table 1 summarizes the input conditions for the cases shown in Figs. 4 through 9. The wind (ϕ) and wave directions are measured counter-clockwise from shore normal. The input peak wave direction, θ, and peak spectral period, T_p, were measured at the 8-m array. The peak wave parameters best represent the dominant wave characteristics. Fig. 2 shows considerable spread in the directional distribution of wave energy, which could strongly influence longshore currents, but has less effect on cross-shore currents. The input wave height was taken from the most seaward of the nine nearshore pressure gages (4-m depth), and the height was inversely refracted and shoaled to the 8-m depth to correspond to the wave direction and period inputs. The height measured at the 8-m array caused a 15% overprediction of the wave height at the most seaward pressure gage, which may be attributable to the use of linear refraction and shoaling in the model. The tide and wind measurements were made at the FRF pier and are averaged values over the sled deployment. For these cases, the sled was deployed spanning low tide to minimize the effect of varying tide elevation.

Table 1. Model input conditions for sample results.

Date	Time	H_{rms} (m)	θ (deg)	T_p (sec)	Tide (m)	W (m/s)	ϕ (deg)
10/17	1000	0.54	-15.0	9.7	-0.47	7.8	130.5
10/18	1100	0.57	-43.0	5.6	-0.62	11.9	79.7
10/19	1200	0.65	24.0	7.0	-0.48	9.1	-51.9

The model results are compared to the field measurements in Figs. 4, 6, and 8 for the cases listed in Table 1. The figures show the measured wave height from the cross-shore array (x), calculated wave height (solid line), calculated setup (chain-dot line),
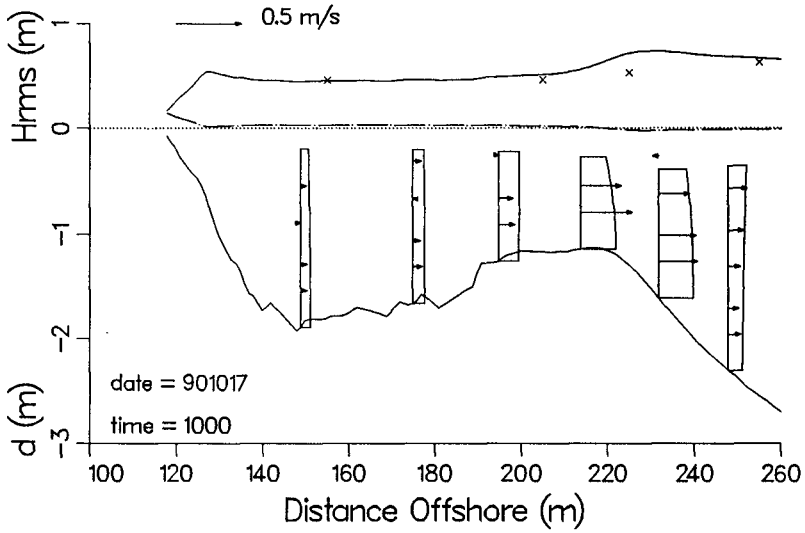
Figure 4. Model results versus measurements (17 October 1990).
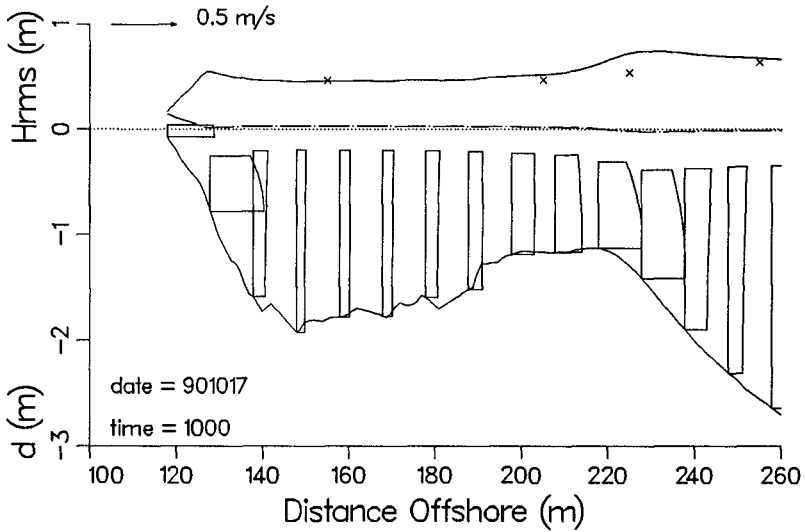
Figure 5. Model results (17 October 1990).
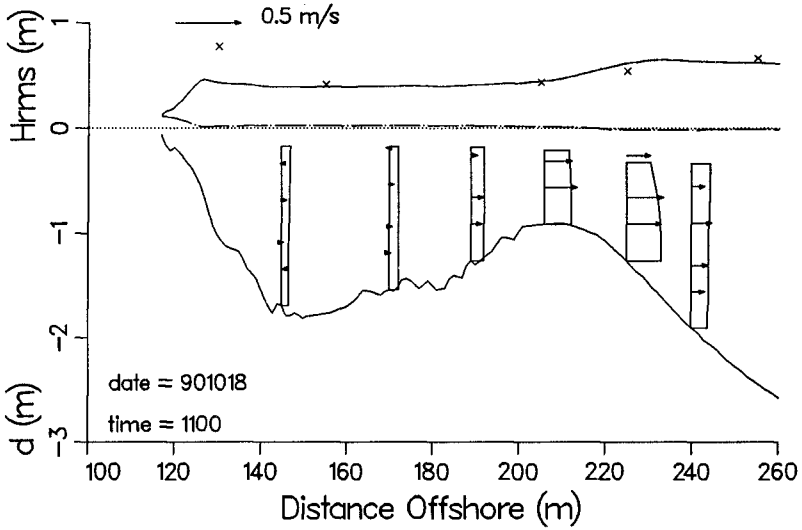
Figure 6. Model results versus measurements (18 October 1990).
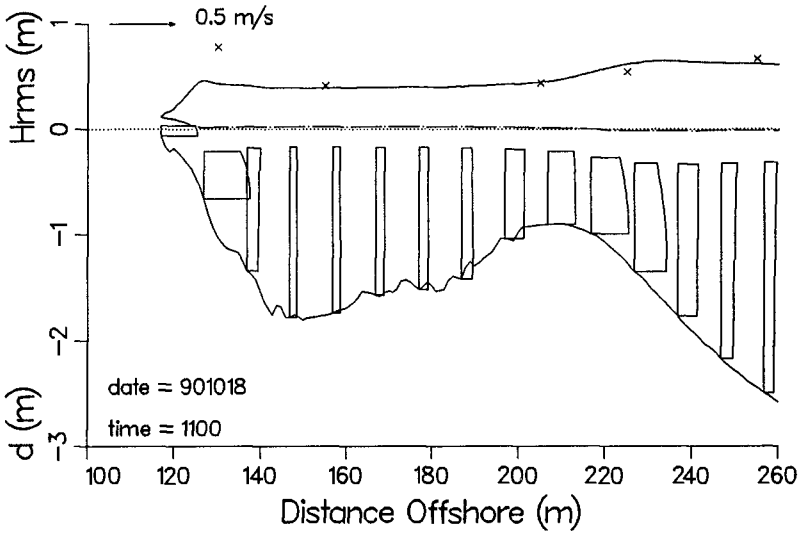
Figure 7. Model results (18 October 1990).
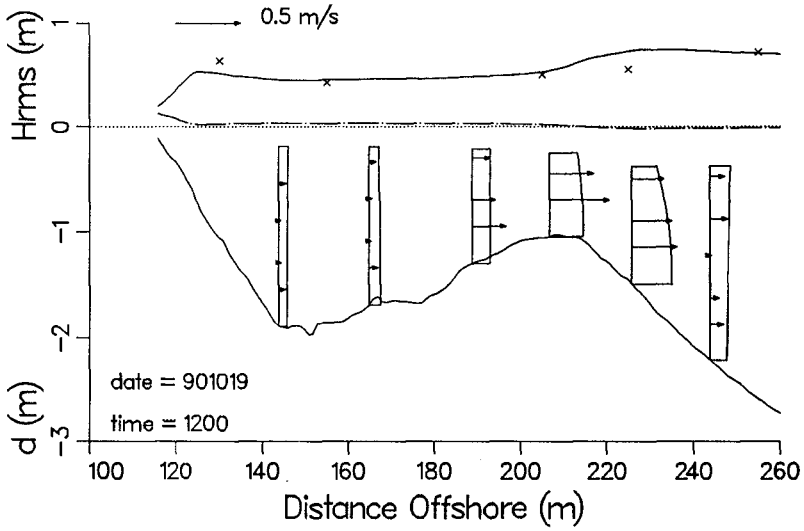
Figure 8. Model results versus measurements (19 October 1990).
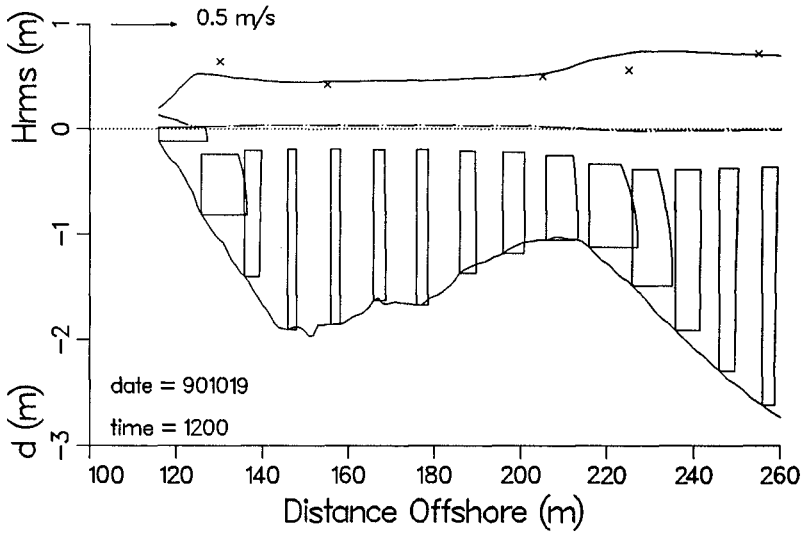
Figure 9. Model results (19 October 1990).

measured cross-shore current from the sled (vectors), and the calculated cross-shore current at the sled positions. Figs. 5, 7, and 9 show the calculated cross-shore current at 10-m intervals to show the cross-shore variation of the undertow profile. Offshore of the breaker zone, the profiles are fairly uniform over depth with a small increase in the offshore velocity near the wave trough level. In the region of rapid wave decay, on the bar crest, the profiles show a characteristic parabolic shape with highest velocities near the bed and smaller velocities at the wave trough. Shoreward of the bar, the waves have reformed and the current profiles are uniform over depth. The cross-shore velocities are low shoreward of the bar. The waves break again on the steep foreshore, and the velocity profiles are similar to those on the bar.

For all cases, the bottom friction factor was set to a constant value of 0.01 and the eddy viscosity to a value of 0.05. The model is relatively insensitive to value of the bottom friction factor, but the shape of the undertow profiles is sensitive to the value of eddy viscosity. Theoretically, the value of the eddy viscosity should be lower in regions of low turbulence (no wave breaking) and higher in regions of intense turbulence (breaker zone), but since the relationship between eddy viscosity and the model parameters is not well known, a constant value was applied. Although the wind speeds were significant during the measurements (8 to 12 m/sec), the wind had very little influence on the results. For the three cases listed in Table 1, the maximum difference in undertow velocity between with- and without-wind simulations was 0.005 m/sec and the root-mean-square (RMS) difference was 0.0012 m/sec.

The RMS error in the cross-shore current results for the 3 cases shown was 5.9 cm/sec. The errors were smallest offshore of the crest of the bar. In the bathymetry trough, the measured velocities were generally 0 to 5 cm/sec, and the RMS error was of the same order. This is not surprising since the low velocities are near the accuracy of the instruments and are susceptible to contamination from the longshore currents which are strong in the trough. The largest RMS errors occurred on the top of the bar (3 to 15 cm/sec), where the model tended to underpredict the measurements, although the model predicted the shape of the undertow profile well. The model results (Figs. 5, 7, and 9) show the maximum undertow velocities just seaward of the crest of the bar, while the measurements show the maximum velocities at the crest of the bar. Errors in the calculation of the wave height may contribute to the underprediction of the undertow at the bar crest (errors in wave height are magnified by squaring the wave height to calculate radiation stress). Also, previous laboratory experiments have shown a shoreward shift in the initiation of setup (the driving force in the model) in the transition region of breaking waves (Svendsen 1984; Roelvink and Stive 1989). This same effect may account for the underprediction of the undertow at the bar crest. Unfortunately, the measurements are not dense enough in the region of the bar crest to resolve this issue.

CONCLUSIONS

Comprehensive measurements of the vertical current structure and the wave and wind forcing were made during the DELILAH field project in October of 1990 on a barred beach bathymetry. The measurements show strong offshore velocities over the bar (0.5 m/sec), and vertical structure of the current was generally parabolic. In the bathymetry trough, the offshore current was weak (0 to 0.05 m/sec) and the structure was uniform over depth. Offshore of the bar, the current was fairly uniform over depth (0.10 to 0.15 m/sec)

to 0.15 m/sec) with a small increase in velocity near the wave trough.

The numerical model developed to calculate the cross-shore (1-D) random wave transformation and vertical current structure compared well with the measurements. The RMS error in prediction of the current was 5.9 cm/sec. The model represented the shape of the vertical current structure well, but tended to underpredict the current magnitude at the bar crest.

ACKNOWLEDGMENTS

REFERENCES

Birkemeier, W. A., and Mason, C. (1984). The CRAB: a unique nearshore research vehicle. *J. Surveying Engrg.*, 1-7.

Dally, W. R., Dean, R. G., and Dalrymple, R. A. (1985). Wave height variation across beaches of arbitrary profile. *J. Geophys. Res.*, 90(C6), 11917-11927.

Hansen, J. B., and Svendsen, I. A. (1984). A theoretical and experimental study of undertow. *Proc. 19th Coastal Engrg. Conf.*, ASCE, 2246-2262.

Larson, M., and Kraus, N. C. (1991). Numerical model of longshore current over bar and trough beaches. *J. Wtrway., Port, Coast., and Oc. Engrg.*, ASCE, 117(4), 326-347.

Longuet-Higgins, M. S., and Stewart, R. W. (1964). Radiation stress in water waves; a physical discussion with applications. *Deep Sea Res.*, 11(4), 529-562.

Putrevu, U., and Svendsen, I. A. (1991). Wave induced nearshore currents: a study of the forcing, mixing and stability characteristics. *Research Report No. CACR-91-11*, Center for Applied Research, University of Delaware.

Putrevu, U., and Svendsen, I. A. (1992). A mixing mechanism in the nearshore region. *Proc. 23rd Coastal Engrg. Conf.*, ASCE, this volume.

Roelvink, J. A., and Stive, M. J. F. (1989). Bar-generating cross-shore flow mechanisms on a beach. *J. Geophys. Res.*, 94(C4), 4785-4800.

Stive, M. J. F., and de Vriend, H. J. (1987). Quasi-3D nearshore current modelling: wave-induced secondary current. *Proc. Coastal Hydrodynamics*, ASCE, 356-370.

Svendsen, I. A. (1984). Wave heights and set-up in a surf zone. *Coastal Engrg.*, 8, 303-329.

Svendsen, I. A., and Hansen, J. B. (1988). Cross-shore currents in surf-zone modelling. *Coastal Engrg.*, 12, 23-42.

Svendsen, I. A., and Putrevu, U. (1990). Nearshore circulation with 3-D profiles. *Proc. 22nd Coastal Engrg. Conf.*, ASCE, 241-254.

Svendsen, I. A., and Putrevu, U. (1992a). Surf-zone wave parameters from experimental data. *Coastal Engrg.*, in press.

Svendsen, I. A., and Putrevu, U. (1992b). Nearshore mixing and dispersion. Submitted for publication.

WAMDI Group (1988). The WAM model: a third generation ocean wave prediction model. *J. Physical Oceanography*, American Meteorological Society, December, 1775-1810.